Journal of Applied Polymer Science

Feldspar/Titanium Dioxide/Chitosan as a Biophotocatalyst Hybrid for the Removal of Organic Dyes from Aquatic Phases

Maryam Yazdani,[1,2] Hajir Bahrami,[1] Mokhtar Arami[1]

[1]Textile Engineering Department, Amirkabir University of Technology, Tehran, Iran

[2]Department of Civil and Environmental Engineering, School of Science and Technology, Aalto University, P.O. Box 15200, FI-00076 Aalto, Finland

Correspondence to: M. Arami (E-mail: arami@aut.ac.ir)

ABSTRACT: Feldspar/titanium dioxide/chitosan hybrid, a photoactive biocompatible adsorbent for anionic dyes, was synthesized, characterized, and successfully tested. The adsorbent characterization, pH role, adsorbent dose effect, equilibrium data, kinetic plats, and thermodynamic parameters are reported. The point of zero charge for the hybrid was measured to be 8.3, and the most favorable pH range for the adsorption process was found to be below this pH value. The adsorption equilibrium study demonstrated that the Freundlich model was best fitted to the experimental data. Without UV light exposure, the prepared adsorbent adsorbed 72 mg of Acid Black 1 (AB1)/g of sorbent (86% removal) from a 100-mL solution with an initial dye concentration of 50 mg/L, whereas UV irradiation resulted in an increase in the elimination of AB1 dye (97% removal). The kinetic data was depicted well by the pseudo-second-order model. The thermodynamic parameters indicated that the reaction between the hybrid and the dye was exothermic and also spontaneous at lower temperatures. In the batch desorption process, several aqueous solutions adjusted to different pH values were tested, and the best desorption performance (90% desorption) was achieved at pH 11. © 2013 Wiley Periodicals, Inc. J. Appl. Polym. Sci. **2014**, *131*, 40247.

KEYWORDS: adsorption; biopolymers and renewable polymers; dyes/pigments; kinetics

Received 4 August 2013; accepted 28 November 2013

DOI: 10.1002/app.40247

INTRODUCTION

In today's industrial world, environmental protection is an important issue. One of the most severe growing problems is water pollution; the contamination of water bodies by a variety of pollutants has been the beginning of an era for effective contamination abatement. Among many industrial wastes discharged into water streams, dyestuffs have been the focus of many recent studies. Because colored wastewaters cause an unpleasant lasting color and extreme chemical oxygen demand loading in water streams, they bring about detrimental environmental damage. Most of these colored compounds are considered hazardous and toxic to many aquatic organisms and may result in the direct destruction of these creatures. Thus, many countries have developed a strict policy of removing these contaminants from dye effluents, and dye-using industries have been pressurized to decolorize their wastewaters before releasing them into the environment. Among available techniques for dye removal, adsorption is preferred because of its potential for removing a variety of coloring agents.[1–7] Moreover, an increase in the possibility of removal could be attained with a combined photocatalytic setup. Many investigations into the integration of these two systems into a hybrid process have achieved promising outcomes.[5,8–10]

Many studies have focused on the attainment of low-cost, locally available adsorbents, including clays, minerals, and sandstone.[11–17] Among different kinds of geological materials, feldspars are the most plentiful and important group of rock-forming minerals; they form approximately 60% of the Earth's crust. Because of both their natural abundance and sorptive quality, feldspars can be brought into economical environmental processes, especially in the removal of contaminants from water and wastewater.[13–15] However, feldspars have little affinity toward anionic species. Therefore, the surface of feldspar should be modified to improve its anion adsorption capacity.

Recently, chitosan (CTS) has been observed for its high adsorption capacity of anionic dyes. CTS is the deacetylated form of chitin and has elevated amounts of amino and hydroxyl groups, which play the roles of coordination and reaction sites and present the additional attractions of being abundant, inexpensive, nontoxic, hydrophilic, biocompatible, and biodegradable.[5,9,18,19] In acidic solution, the amino groups of CTS are easily protonated and bounded anionic species.[3,5,20] Even

though CTS shows excellent adsorption capacities, its unfavorable mechanical properties and its low specific gravity make it rather inconvenient for the use as an adsorbent in batch and column treatment systems. Thus, CTS composites have been developed to eliminate contaminants from wastewater because they have been proven to possess better resistance to acidic environments.[6,21–24] In addition, CTS has demonstrated multifunctional performances with titanium dioxide (TiO_2) in photocatalysis techniques through the intensification of the adsorption–photocatalytic system. TiO_2 is a well-known photocatalyst that is widely used for the degradation of organic pollutants under UV irradiation in water and wastewater treatment. When TiO_2 particles are irradiated by UV light, the excitation of electrons takes place from the valence band to the conduction band, and the hole–electron pairs are brought forward. Afterward, organic contaminants are oxidized by photogenerated holes or by active oxygen forms such as $OH^{\bullet}$ and $O_2^{\bullet-}$ radicals generated by the interaction of electrons, H_2O, O_2, and so on, on the irradiated surface of TiO_2 particles.[25] Generally, the adsorption–photocatalytic mechanism for anionic dyes indicates that the incorporation of CTS polyelectrolyte at the surface of the TiO_2 particles creates a synergistic effect by enhancing the adsorption capacity because of the charge interaction with dye anions.[8,25,26]

It was expected that feldspar, CTS, and TiO_2 could complement each other with their own advantages and, hence, present a comprehensive way of removing various water and wastewater pollutants. Thus, in this study, a feldspar/TiO_2/CTS composite was prepared and characterized in detail. Acid Black 1 (AB1) dye was selected as the object pollutant in the examination of the adsorption and photocatalytic efficiency of the new catalyst. The effects of different factors on the adsorption process are also reported. Also, it was very absorbing to analyze the combined effects of adsorption–photodegradation provided by the prepared composite, and this was one of the major aims of this study. The adsorption properties, such as the equilibrium, kinetics, and thermodynamics, were investigated by batch experiments. Lastly, a desorption study was conducted to evaluate the adsorbent regeneration.

EXPERIMENTAL

Chemicals

CTS (degree of deacetylation = 85%; average molecular weight = 1000 kD) was supplied by Chitotech Co. (Iran). AB1 presented in Figure 1 was provided by Ciba, Ltd., and was used without purification. The photocatalyst we used was commercial TiO_2 Degussa (P-25) supplied by Tecnon Co. (Spain). According to the manufacturer's specifications, P-25 had an elementary particle size of 30 nm, and its crystalline mode was 80% anatase and 20% rutile. The local feldspar was provided from Hamedan, Iran. All other chemicals were purchased from Merck (Germany).

Preparation of the Feldspar/TiO_2/CTS Hybrid

An amount of 2.5 g of CTS was dissolved in a premixed solution of 200 mL of 0.1*M* CH_3COOH and 50 mL of 0.2*M* NaCl. The viscous solution was stirred continuously for 24 h to fully dissolve the CTS. Then, 1.25 g of TiO_2 powder was slowly added to the viscous solution. The mixture was stirred steadily for another 24 h. An amount of 1.25 g of the feldspar mineral was immersed in 50 mL of distilled water overnight. The former solution was slowly added to feldspar suspension, and this was followed by stirring for 2 days. The composite was formulated by the dispersal of the solution into 0.1*M* NaOH (10 mL of CTS solution/40 mL of NaOH). The composite was immersed in 0.1*M* NaOH overnight and was then filtered and rinsed with deionized water until the filtrate was of neutral pH. Finally, the sample was allowed to dry in the hood and was ground and sieved.

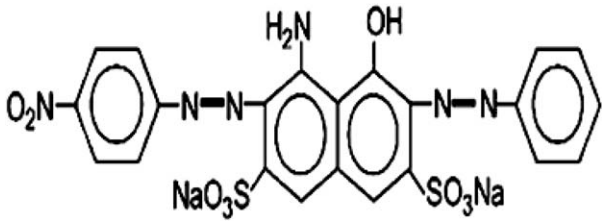

Figure 1. Chemical structure of AB1.

Characterization of the Feldspar/TiO_2/CTS Hybrid

The Fourier transform infrared (FTIR) spectra of the precursor materials and the prepared feldspar/TiO_2/CTS composite were obtained by the use of a PerkinElmer Spectrum One spectrophotometer within 450–4000 cm^{-1}. X-ray diffraction (XRD) was performed on a Philips PW 1800 powder diffractometer. Scanning electron microscopy (SEM) was conducted to analyze the morphology of the samples.

Determination of the Point of Zero Charge (pH_{pzc})

The pH at which the total surface charge of the absorbent is zero is referred to pH_{pzc}.[21] To determine the pH_{pzc} of the feldspar/TiO_2/CTS composite, the pH drift method was applied with 20 mL of 0.1*M* NaCl in a series of solutions whose pH was adjusted with 0.1*M* HCl and 0.1*M* NaOH within the range 3–11. After we determined the initial pH of the solutions, 0.025 g of the adsorbent was added to each of them, and their final pH was measured after 24 h. pH_{pzc} was considered to be the pH at which the initial pH was equal to the final pH.[21]

Batch Adsorption Experiments

We conducted all of the experiments by mixing 0.06 g of adsorbent with 100 mL of aqueous solution of dye with the desired concentration, pH, and temperature and agitating the mixture for 3 h at 150 rpm. The pH of the dye solutions was adjusted to different pH values within 4–11 with HCl or NaOH solutions. For the equilibrium experiments, 100 mL of various initial AB1 concentrations (from 10 to 150 mg/L) were mixed with 0.06 g of feldspar/TiO_2/CTS and then agitated at the desired temperature until equilibrium was established. Initial dye concentrations of 30, 50, 70, and 90 mg/L were used to study the adsorption kinetics, and the AB1 concentrations were monitored at different interval times until the adsorption process reached equilibrium. The equilibrated solutions were taken out, and the adsorbent was separated from them with a centrifuge. The concentration of the dye in the residual solution was determined with a UV–vis spectrophotometer at 618 nm. The

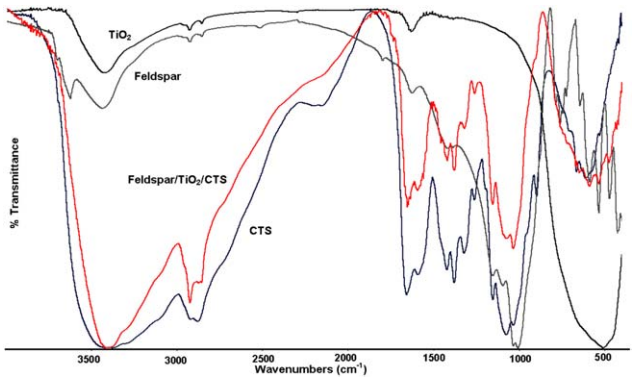

Figure 2. FTIR spectra of feldspar, CTS, TiO_2, and the feldspar/TiO_2/CTS hybrid. [Color figure can be viewed in the online issue, which is available at wileyonlinelibrary.com.]

adsorption capacity [qe (mg/g)] of the adsorbents for AB1 was determined with the following equation:

$$q_e = \frac{(C_0 - C_e)V}{M} \quad (1)$$

where C_e and C_0 represent the final and initial concentrations (mg/L) of AB1 in solution, respectively, and M and V are the adsorbent weight (g) and the solution volume (L), respectively.

Photocatalysis Studies

In the photocatalysis experiments, the experimental setup was similar to that in the adsorption experiments, except that the solutions were irradiated with a 9-W Phillips UV lamp. The experiments were carried out in a custom-made photodegradation–adsorption reactor, as illustrated in Figure 2. The solution was sealed from incoming light but illuminated by the light source at the center of the solution reservoir.

Desorption Experiments

The feldspar/TiO_2/CTS used for the treatment of the 100 mg/L dye solution was separated from the mixture by centrifugation. The spent adsorbent was collected and gently washed with distilled water to get rid of any unadsorbed color. After the preparation of several such samples, the dye-loaded adsorbent was agitated with 100 mL of distilled water and adjusted to different pH values for 3 h. The desorption efficiency was determined as follows:

$$\text{Desorption } (\%) = \frac{C_d \times V_d}{w \times q_e 1000} \times 100 \quad (2)$$

where C_d is the desorbed dye concentration (mg/L), V_d is the volume of the desorption solution, w is the mass of the preadsorbed adsorbent (g), and q_e is the amount of the adsorbate preadsorbed on the adsorbent (mg/g).

RESULTS AND DISCUSSION

Characterization of the Feldspar/TiO2/CTS Hybrid

FTIR Spectra. The FTIR spectra for the precursor materials and the newly synthesized composite are presented in Figure 2. From the spectra of feldspar, the band at 3623 cm^{-1} and the broad band around 3430 cm^{-1} were attributed to the Al_2OH groups of the octahedral layer and the —OH stretching vibrations of water molecules on the external layer of feldspar, respectively. Also, the band around 1000 cm^{-1} was related to the stretching vibrations of the Si—O groups, whereas the peaks at 523 and 465 cm^{-1} were due to Al—O—Si and Si—O—Si bending vibrations, respectively.[14] The FTIR spectrum of CTS displayed the peaks of the amine (—NH_2) and hydroxyl (—OH) groups at 1654 and 3436 cm^{-1}, respectively.[5,8] These functional groups on the structure of CTS could act as reaction sites for the adsorption of pollutants.[8] In the region 700–500 cm^{-1}, TiO_2 revealed a large broad band contributing to the stretching vibration of Ti—O—Ti around 500 cm^{-1} and to the bending vibration band of Ti—O and O—Ti—O around 600 cm^{-1}.[27]

However, the spectrum of the feldspar/TiO_2/CTS presented an intriguing characteristic of the precursor materials. The absorption bands at 1400, 1580, 2865, and 3400 cm^{-1} were due to the binding of hydroxyl groups, among which the peak at 2865 cm^{-1} was a sign of surface TiO_2—OH groups. The peaks at 1260, 1319, and 1654 cm^{-1} were assigned to the amine or amide functional groups. In addition, the existence of TiO_2 nanoparticles was reaffirmed by the appearance of the band around 600 cm^{-1}. This evident existence of the TiO_2 compound along with the hydroxyl, amide, and amine functional groups could help to ensure the effective removal of the dye molecules via a photodegradation–adsorption mechanism.

XRD Analysis. Figure 3 displays the XRD patterns of the feldspar, TiO_2, and feldspar/TiO_2/CTS hybrid. As the XRD pattern of the feldspar/TiO_2/CTS showed, the peaks corresponding to the anatase TiO_2 phase appeared at $2\theta = 24.9$, 37.4, and 47.5°.

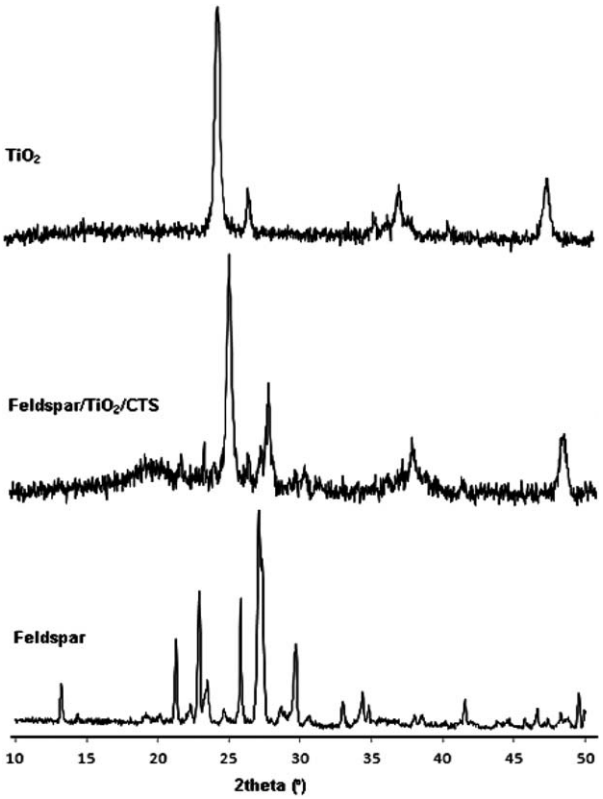

Figure 3. XRD patterns of feldspar, TiO_2, and feldspar/TiO_2/CTS.

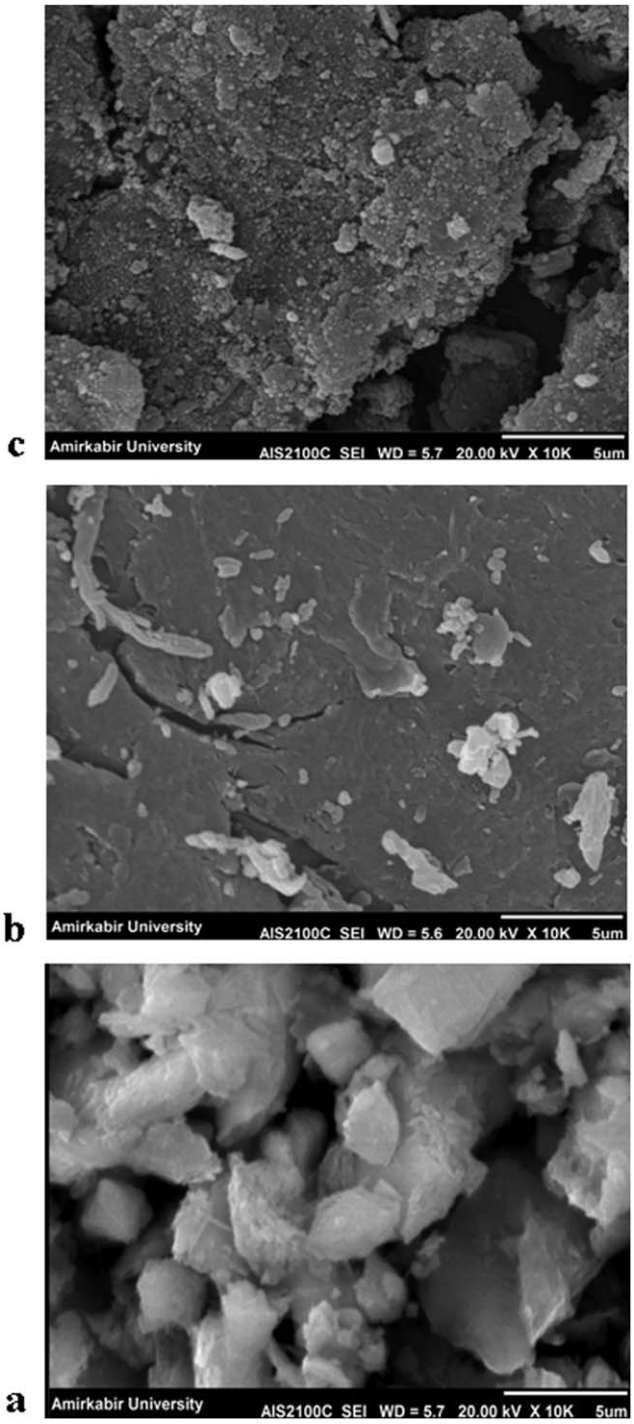

Figure 4. SEM images of (a) feldspar, (b) CTS, and (c) feldspar/TiO_2/CTS.

It was evident that the major phase of synthesized composite was predominantly anatase. However, rutile peaks also occurred at 27.5°, and this existence of the rutile phase may have been harmful to the photoactivity.[8] Compared with the XRD pattern of the feldspar, the pattern of feldspar/TiO_2/CTS showed some changes between 2θ values of 18.00 and 40.00°; this suggested the intercalation of feldspar. Moreover, the significant intensity decreased, and slight shifts at $2\theta = 21$, 23, 26.66, and 35.34°, observed as broadenings in the hybrid pattern, were attributable to delamination and disorientation of the mineral platelets.[28]

SEM Image Analysis. The SEM images of the feldspar, CTS, and feldspar/TiO_2/CTS hybrid are shown in Figure 4. We observed that the structure of the feldspar particles consisted of a crystalline and irregular layered structure, whereas CTS displayed a relatively smooth structure with some cracks on the surface. We observed that there was a significant difference in the surface morphology of the precursor materials and newly synthesized hybrid. Figure 4(c) confirms the presence of many pores and cracks on the irregular and rough surface of the feldspar/TiO_2/CTS, which could supply a larger surface area for the photocatalytic reaction.

Role of pH and pH_{pzc}

The pH of the dye solution was a major controlling factor in the existence of a strong effect on the adsorption capacity of the feldspar/TiO_2/CTS hybrid. Figure 5 illustrates the adsorption of AB1 against the pH of the solution. The maximum adsorption of the dye ions on the hybrid were found at pH 4. The pH_{pzc} was found at approximately 8.3 (Figure 5); this was a sensible result because the pH_{pzc} values for feldspar and TiO_2 have been reported as 7.5[14] and 6.9,[29] respectively, and the pK_a values of CTS varies from 6.3 to 7.2[30] and is contingent on features such as the degree of acetylation and ionic strength.[20] At pH values greater than pH_{pzc}, the surface of feldspar/TiO_2/CTS was negatively charged; on the other hand, the surface of the hybrid was positively charged at pH values lower than pH_{pzc}. Therefore, there was an increase in the adsorption at pH values lower than pH_{pzc} because of the electrostatic interaction of dye anions with the positively charged surface of the sorbent.

Effect of the Adsorbent Dosage

The effect of the adsorbent concentration on the adsorption process of AB1 is presented in Figure 6. As expected, the removal percentage of AB1 increased as the hybrid dose increased. However, the adsorption density [q (mg/g)] decreased

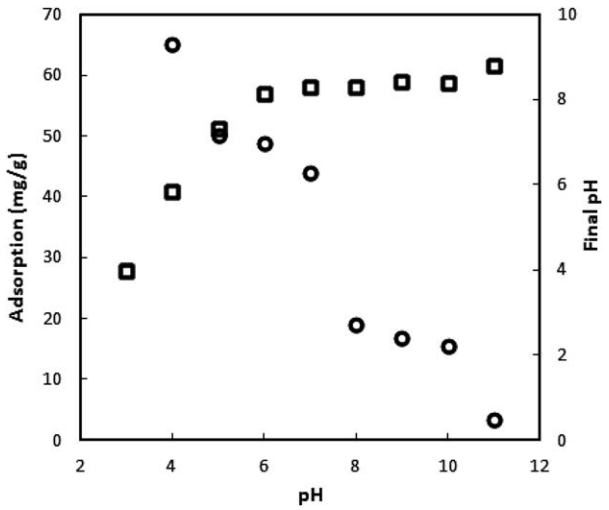

Figure 5. Effect of pH on the adsorption of AB1 on feldspar/TiO_2/CTS: (○) adsorption (mg/g) and (□) final pH (initial dye concentration = 50 mg/L, agitation speed = 200 rpm, and temperature = 25°C).

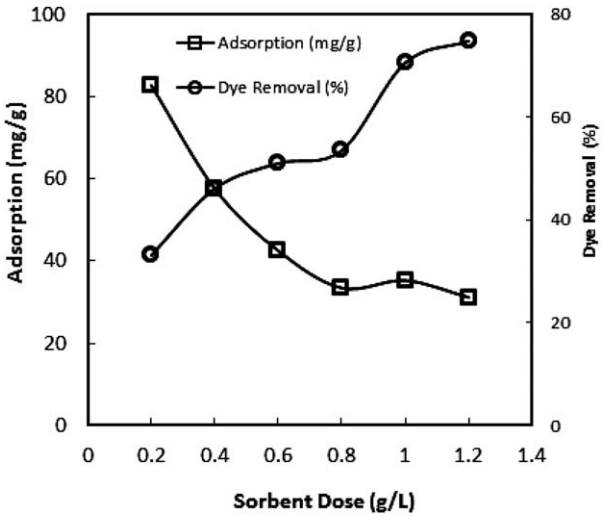

Figure 6. Effect of the adsorbent dosage on the AB1 removal (initial dye concentration = 50 mg/L, natural pH, agitation speed = 200 rpm, and temperature = 25°C).

with increasing adsorbent dose. For an increase from 0.2 to 1.2 g/L in the concentration of the sorbent, the calculated percentage of adsorption enhanced from 33 to 75%, whereas q decreased from 83 to 31 mg/g. The increase in the dye uptake could be described by the availability of more sorption sites with the enhancement in the biobased composite mass. On the other side, the decrease in q was due to the concentration gradient between the dye molecules with increasing sorbent dose, which resulted in a decrease in the dye adsorbed on the unit mass of the adsorbent. Furthermore, the interaction between adsorbent particles, for example, aggregation, caused by the high adsorbent dosage could lead to a decrease in the total surface area of the sorbent and consequently q.[31]

Adsorption Equilibrium

The Freundlich[32] and Langmuir isotherm models[33] for the adsorption of the AB1 dye onto the feldspar/TiO_2/CTS hybrid

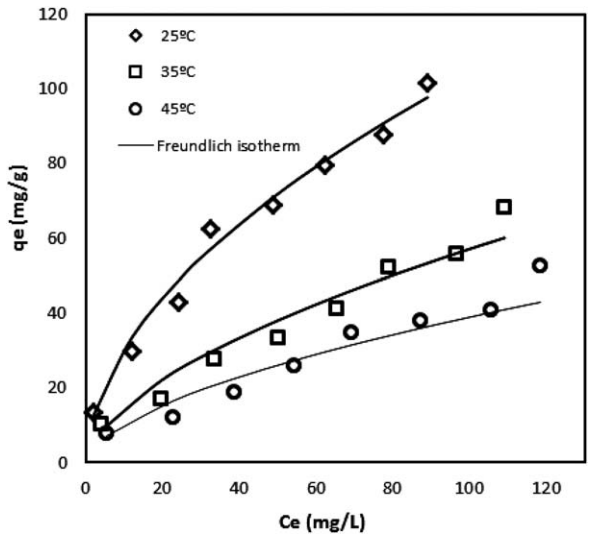

Figure 7. Isotherm models for the adsorption process of AB1.

Table I. Isotherm Constants for AB1 Dye Adsorption onto Feldspar/TiO_2/CTS

		Temperature (°C)		
Isotherm model	Constant	25	35	45
Freundlich	K_F	8.93	3.86	2.72
	$1/n$	0.53	0.58	0.59
	R^2	0.99	0.96	0.93
Langmuir	q_{max}	76.92	50	34.48
	K_L	0.11	0.06	0.06
	r^2	0.94	0.88	0.84

are displayed in Figure 7. In addition, the equilibrium characteristics of the AB1 adsorption at three temperatures are also detailed in Table I.

The Freundlich model relating the adsorption onto a heterogeneous surface is commonly displayed by

$$\log q_e = \log K_F + 1/n \log C_e \tag{3}$$

where K_F and $1/n$ are the Freundlich constants representing the adsorption capacity (mg/g) and adsorption intensity of the prepared adsorbent, respectively.

Used to depict monolayer adsorption on the surface with a finite number of identical sites, Langmuir theory assumes uniform adsorption on the surface. The linear Langmuir equation is expressed as follows:

$$\frac{1}{q_e} = \frac{1}{q_{max} K_L C_e} + \frac{1}{q_{max}} \tag{4}$$

where K_L and q_{max} are the affinity constant and the maximum adsorption capacity of the adsorbent, respectively. As observed

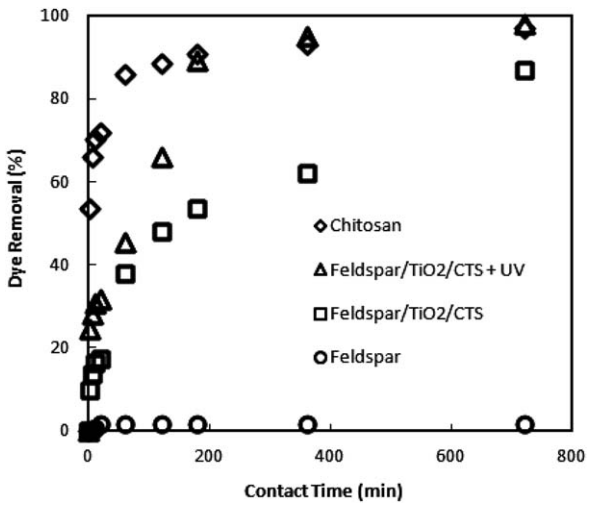

Figure 8. Time variation of AB1 removal for AB1 solutions with (◇) CTS, (○) feldspar, (□) feldspar/TiO_2/CTS without UV irradiation, and (△) feldspar/TiO_2/CTS under UV irradiation.

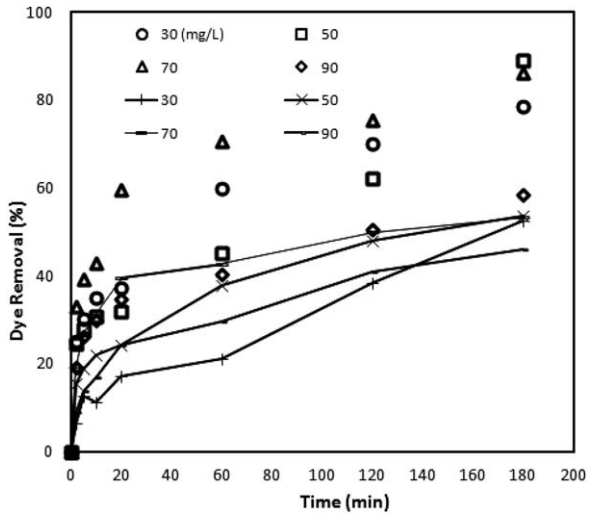

Figure 9. Kinetic plots for AB1 adsorption onto feldspar/TiO_2/CTS in the absence of UV light (30, 50, 70, and 90 mg/L) and in the presence of UV light (30, 50, 70, and 90 mL/L). The presented data are aggregates of two separate batch experiments conducted at 25°C and 200 rpm with a UV lamp (9 W).

from Figure 8, the Freundlich model fits the adsorption equilibrium data better than the Langmuir model. This phenomenon may have been due to the heterogeneous distribution of active sites on the surface of the feldspar/TiO_2/CTS hybrid, as the Freundlich isotherm assumes a heterogeneous surface for the adsorbent. From Table I, it is evident that the constants K_F and $1/n$ were influenced by the temperature. When the temperature was increased from 25 to 45°C, the values of K_F decreased (from 8.93 to 2.92); the adsorption capacity of the hybrid also decreased. This suggested that the nature of dye uptake by the hybrid was an exothermic process. Furthermore, the values of $1/n$, which varied between 0 and 1, depicted a favorable adsorption process.[14] An increase in the temperature also caused an increase in the $1/n$ values (from 0.53 to 0.59); this pointed out the decreasing intensity of adsorption, which was in confirmation with the Freundlich model constants.[34]

Role of UV Irradiation

It is widely reported that CTS and its derivatives show a strong tendency to absorb trace organic contaminants from aqueous solutions[8,20] and TiO_2 can catalyze the photooxidation of organic compounds in water phases.[5,8–10] The feldspar/TiO_2/CTS hybrid, presented in this report, combined the adsorptive capacity of the CTS/feldspar with the ability of TiO_2 to effectively photooxidize AB1. To analyze the photocatalytic properties of the newly synthesized hybrid, a set of kinetic data was scrutinized.

According to Figures 8 and 9, it was obvious that feldspar/TiO_2/CTS represented greater AB1 removal in the presence of UV light than in the absence of UV light. Figure 8 indicates a comparative study of AB1 removal with CTS, feldspar, and feldspar/TiO_2/CTS in the absence of UV light and also feldspar/TiO_2/CTS in the presence of UV light. This allowed us not only to compare the adsorption ability of the starting materials and prepared adsorbent but also to estimate the contribution of both AB1 absorption and photolysis by the feldspar/TiO_2/CTS. Without UV irradiation, the feldspar/TiO_2/CTS hybrid showed a much higher adsorption capacity than feldspar. The adsorption capacity of the hybrid was found to be a little less than that of CTS. However, in the presence of UV light, the dye removal by feldspar/TiO_2/CTS increased and reached the amount of dye removed by CTS. It increased from 86 to 97%. This was the result of the simultaneous occurrence of the adsorption and photocatalysis processes. With exposure to UV light, AB1 removal increased significantly for all concentrations of the solutions, as shown in Figure 9. This outcome may be hopeful for trace organic treatment because sunlight, an easily obtainable source of UV light, can be used to improve the removal process.

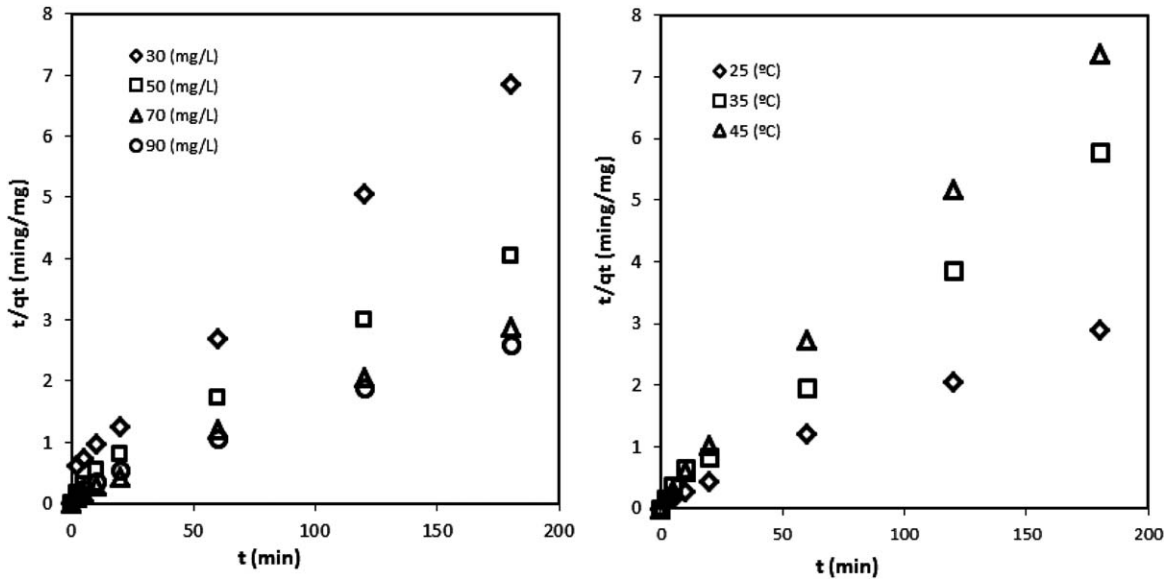

Figure 10. Pseudo-second-order kinetic model for AB1 at (a) different dye concentrations and (b) different temperatures.

Table II. Kinetic Constants for the Pseudo-First-Order Model and the Pseudo-Second-Order Model

Temperature (°C)	Concentration (mg/L)	$q_{e,exp}$ (mg/g)	Pseudo-first-order model			Pseudo-second-order model		
			$q_{e,1}$ (mg/g)	k_1 (min^{-1})	r^2_1	$q_{e,2}$ (mg/g)	k_2 (g mg^{-1} min^{-1})	r^2_2
25	30	22.29	29.51	0.04	0.86	27.03	0.003	0.99
	50	44.64	58.88	0.05	0.80	46.29	0.002	0.99
	70	62.22	57.54	0.04	0.85	63.29	0.016	0.99
	90	68.92	97.72	0.05	0.81	71.42	0.001	0.99
35	30	17.14	10.94	0.53	0.87	17.24	0.014	0.99
	50	37.41	20.40	0.06	0.94	32.15	0.006	0.99
	70	45.24	36.02	0.04	0.78	44.64	0.005	0.99
	90	50.74	53.49	0.04	0.85	51.55	0.002	0.99
45	30	12.03	6.41	0.02	0.84	12.03	0.013	0.99
	50	18.65	16.45	0.04	0.78	18.28	0.010	0.99
	70	24.41	15.20	0.04	0.87	24.39	0.012	0.99
	90	37.92	33.09	0.05	0.85	38.17	0.005	0.99

Adsorption Kinetics

Two kinetic models, pseudo-first-order[35] and pseudo-second-order,[36] were chosen to investigate the adsorption process. The first-order kinetic model equation can be represented as follows:

$$\log(q_{e,1}-q_t)=\log(q_{e,1})-\frac{k_1}{2.303}t \quad (5)$$

where k_1 is the pseudo-first-order rate constant (min^{-1}) and $q_{e,1}$ and q_t are the amounts of dye adsorbed (mg/g) at equilibrium and at time t (min).

The pseudo-second-order model is based on the adsorption equilibrium capacity and can be written as follows:

$$\frac{t}{q_t}=\frac{1}{k_2 q_{e,2}^2}+\frac{t}{q_{e,2}} \quad (6)$$

where k_2 is the rate constant of the pseudo-second-order adsorption (g mg^{-1} min^{-1}). The k_1, k_2, $q_{e,1}$, calculated adsorption capacity ($q_{e,2}$), and correlation coefficients r^2_1 and r^2_2 of AB1 adsorption on the composite, calculated from the plots of Figure 10, are listed in Table II. According to the linear regression coefficients ($r^2_2 = 0.99$) and the values of the experimental adsorption capacity ($q_{e,exp}$) and $q_{e,2}$, which were in agreement, the adsorption of AB1 onto the prepared hybrid obeyed the pseudo-second-order model.

Adsorption Thermodynamics

Thermodynamic parameters, such as the free energy change (ΔG^o), enthalpy change (ΔH^o), and entropy change (ΔS^o), were estimated.[16,37,38] The obtained thermodynamic values are summarized in Table III.

ΔG^o is used to distinguish the spontaneity of the adsorption process; the higher the negative value of ΔG^o is, the more energetically favorable the adsorption process will be. ΔG^o for AB1 had a negative sign at 25°C (with dye concentrations of 30, 50, and 70, $\Delta G^o = -0.25$, -0.36, and -0.33 kJ/mol, respectively); this means

Table III. Thermodynamic Parameters for the Adsorption of AB1 onto Feldspar/TiO_2/CTS

C_0 (mg/L)	T (K)	Thermodynamic parameters		
		ΔG (kJ/mol)	ΔH (kJ/mol)	ΔS (J mol^{-1} K^{-1})
30	298	−0.25	−56.32	−188.21
	308	1.67		
	318	3.52		
50	298	−0.36	−54.58	−181.80
	308	1.32		
	318	3.29		
70	298	−0.33	−57.51	−191.42
	308	1.17		
	318	3.52		
90	298	0.40	−36.32	−123.32
	308	1.72		
	318	2.87		

ΔG = free energy change; ΔH = enthalpy change; ΔS = entropy change.

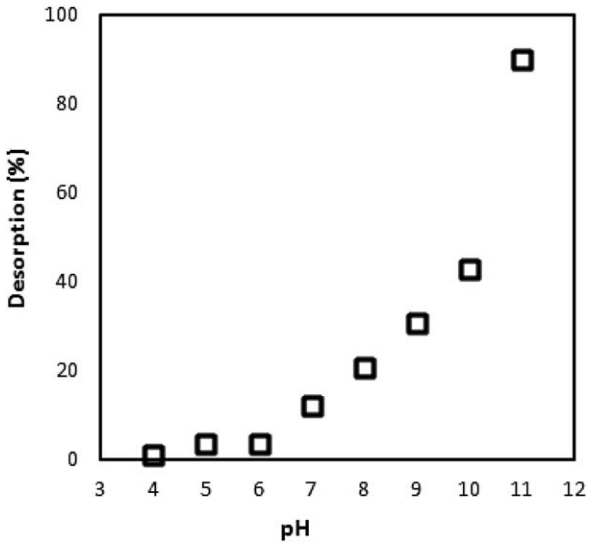

Figure 11. Effect of pH on the AB1 desorption from the dye-loaded composites (adsorbent dose = 0.06 mg/100 mL and temperature = 25°C).

that the AB1 adsorption by feldspar/TiO_2/CTS was spontaneous and could be considered as physisorption.[37] On the contrary, the positive signs of ΔG^o at 35 and 45°C suggest the presence of an energy barrier at higher temperatures in the adsorption, and therefore, adsorption was not spontaneous at these temperatures.[37] Negative values of ΔH^o reveal that the adsorption process is exothermic and was less favorable at higher temperatures. Negative values of ΔS^o indicate that the randomness decreased at the solid–solution interface during adsorption.[37]

Desorption Studies

The economic feasibility of the application of an adsorbent for removing pollutants from water and wastewater is conditioned by its regeneration and reuse. In this study, the spent adsorbent in adsorption process without UV light were used to analyze the desorption process so that in this way, we were able to recycle both the used adsorbent and adsorbate. Figure 11 displays the results of the desorption study. As shown, when the desorbing pH was increased, the percentage of desorption enhanced from 1.2% at pH 4 to 90% at pH 11. On the one hand, we observed that desorption at acidic pH yielded very low dye recovery values of 1.2–3.7%; this demonstrated the stability of the feldspar/TiO_2/CTS hybrid particles in capturing dye ions under acidic conditions. On the other hand, desorption at alkaline pH displayed high dye recovery values of 30–90%. This high level of desorption implied that physisorption might have been the main mode of AB1 removal by the composite.

CONCLUSIONS

A study of innovation of a feldspar/TiO_2/CTS biophotocatalyst was undertaken and combined with the comprehensive characterization of its adsorption properties to develop a photoactive biocompatible sorbent that was capable of eliminating anionic species through a synergistic adsorption–photocatalyst system. We observed that the adsorption of AB1 by the synthesized hybrid was significantly higher than that of feldspar but somewhat lower than that of CTS. However, when the system was exposed to UV light, the adsorption capacity of adsorbent reached that of CTS, whereas feldspar/TiO_2/CTS removed 72 mg of AB1/g of sorbent (86%) in a standard batch experiment (dye concentration = 50 mg/L and temperature = 25°C). It gains 97% removal of the dye when the system was exposed to UV light. Moreover, the pH had a significant effect on the performance of the composite with optimal performance below pH_{pzc}. The Freundlich isotherm model best represents the equilibrium adsorption of AB1. According to kinetic studies, the adsorption process obeyed the pseudo-second-order model. Thermodynamic studies revealed that AB1 adsorption was spontaneous at lower temperatures, exothermic, and consequently less favorable at higher temperatures. Desorption studies also revealed that the best desorption performance (90% desorption) was achieved at pH 11.

ACKNOWLEDGMENTS

The main author thanks Seyed Hossein Amirshahi (Amirkabir University of Technology) for kindly providing the model pollutant.

REFERENCES

1. Grisdanurak, N.; Akewaranugulsiri, S.; Futalan, C. M.; Tsai, W.; Kan, C.; Hsu, M.-W.; Wan, C.-W. *J. Appl. Polym. Sci.* **2012**, *125*, 132.
2. Rodriguez, A.; Ovejero, G.; Mestanza, M.; Garcia, *J. Ind. Eng. Chem. Res.* **2010**, *49*, 3207.
3. Zhu, H.-Y.; Jiang, R.; Xiao, L. *Appl. Clay Sci.* **2010**, *48*, 522.
4. Ahmaruzzaman, M.; Gupta, V. K. *Ind. Eng. Chem. Res.* **2011**, *50*, 13589.
5. Nawi, M. A.; Sabar, S.; Jawad, A. H.; Sheilatina, W. S.; Wan, N. *Biochem. Eng. J.* **2010**, *49*, 317.
6. Ngah, W. S. W.; Ariff, N. F. M.; Hashim, A.; Hanafiah, M. A. K. M. *Clean Soil Air Water* **2010**, *38*, 394.
7. Jiang, R.; Fu, Y.; Zhu, H.-Y.; Yao, J.; Xiao, L. *J. Appl. Polym. Sci.* **2012**, *125*, 540.
8. Zainal, Z.; Kong Hui, L.; Hussein, M. Z.; Abdullah, A. H.; Hamadneh, I. R. *J. Hazard. Mater.* **2009**, *164*, 138.
9. Miller, S. M.; Zimmerman, J. B. *Water Res.* **2010**, *44*, 5722.
10. Dvininova, E.; Popovici, E.; Podeb, R.; Cocheci, L.; Barvinschi, P.; Nica, V. *J. Hazard. Mater.* **2009**, *167*, 1050.
11. Wang, C. C.; Juang, L. C.; Hsu, T. C.; Lee, C. K.; Lee, J. F.; Huang, F. C. *J. Colloid Interface Sci.* **2004**, *273*, 80.
12. Atun, G.; Tunçay, M.; Hisarli, G.; Talman, R. Y.; Hoşgörmez, H. *Appl. Clay Sci.* **2009**, *45*, 254.
13. Aşçl, Y.; Nurbaşa, M.; SağAçıkelb, Y. *J. Environ. Manage.* **2008**, *88*, 383.
14. Yazdani, M.; Mahmoodi, N. M.; Arami, M.; Bahrami, H. *Sep. Sci. Technol.* **2012**, *47*, 1660.
15. Yazdani, M.; Mahmoodi, N. M.; Arami, M.; Bahrami, H. *J. Appl. Polym. Sci.* **2012**, *126*, 340.
16. Karadag, D.; Akgul, E.; Tok, S.; Erturk, F.; Arif Kay, M.; Turan, M. *J. Chem. Eng. Data* **2007**, *52*, 2436.
17. Sadeghi-Kiakhani, M.; Arami, M.; Gharanjig, K. J. *Appl. Polym. Sci.* **2012**, *13*, 2607.
18. Mahmoodi, N. M.; Salehi, R.; Arami, M.; Bahrami, H. *Desalination* **2011**, *267*, 64.
19. Burke, A.; Yilmaz, E.; Hasirci, N.; Yilmaz, O. J. *Appl. Polym. Sci.* **2002**, *84*, 1185.
20. Crini, G.; Badot, P.-M. *Prog. Polym. Sci.* **2008**, *33*, 399.
21. Zou, X.; Pana, J.; Ou, H.; Wang, X.; Guan, W.; Li, C.; Yan, Y.; Duan, Y. *Chem. Eng. J.* **2011**, *167*, 112.
22. Wan Ngah, W. S.; Teong, L. C.; Hanafiah, M. A. K. M. *Carbohydr. Polym.* **2011**, *83*, 1446.
23. Wang, L.; Zhang, J.; Wang, A. *Desalination* **2011**, *266*, 33.
24. Gupta, N.; Kushwah, A. K.; Chattopadhyaya, M. C. J. *Taiwan Inst. Chem. Eng.* **2012**, *43*, 125.
25. Ke Chen, J. L.; Li, J.; Zhang, Y.; Wang, W. *Colloids Surf. A* **2010**, *360*, 47.
26. Li, Q.; Su, H.; Tan, T. *Biochem. Eng. J.* **2008**, *38*, 212.
27. Chen, K.; Li, J.; Li, J.; Zhang, Y.; Wang, W. *Colloids Surf. A* **2010**, *360*, 47.
28. Sarier, N.; Onder, E. *Thermochim. Acta* **2010**, *510*, 113.

29. Dutta, P. K.; Ray, A. K.; Sharma, V. K.; Millero, F. J. *J. Colloid Interface Sci.* **2004**, *278*, 270.
30. Gerente, C.; Lee, V. K. C.; Le Cloirec, P.; McKay, G. *Crit. Rev. Environ. Sci. Technol.* **2007**, *37*, 41.
31. Deng, H.; Lu, J.; Li, G.; Zhang, G.; Wang, X. *Chem. Eng. J.* **2011**, *172*, 326.
32. Freundlich, H. M. F. Z. *Phys. Chem.* **1906**, *57*, 385.
33. Langmuir, I. *J. Am. Chem. Soc.* **1916**, *38*, 2221.
34. Özcan, A.; Özcan, A. S. *J. Hazard. Mater. B* **2005**, *125*, 252.
35. Lagergren, S. *Kungliga Svenska Vetenskapsakademiens Handlingar* **1898**, *24*, 1.
36. Ho, Y. S.; McKay, G. *Process. Biochem.* **1999**, *34*, 451.
37. Karadag, D.; Turan, M.; Akgul, E.; Tok, S.; Faki, A. J. *Chem. Eng. Data* **2007**, *52*, 1615.
38. Jain, S.; Jayaram, R. V. *Desalination* **2010**, *250*, 921.